

## Subcritical excitation of the current-driven Taylor instability by super-rotation

G. Rüdiger,<sup>1,2, a)</sup> M. Schultz,<sup>1,2</sup> M. Gellert,<sup>1</sup> and F. Stefani<sup>2</sup>

<sup>1)</sup>*Leibniz-Institut für Astrophysik Potsdam, An der Sternwarte, 14482 Potsdam, Germany*

<sup>2)</sup>*Helmholtz-Zentrum Dresden-Rossendorf, P.O. Box 510119, D-01314 Dresden, Germany*

(Dated: 10 June 2019)

In a hydrodynamic Taylor-Couette system a rotation law with positive shear (‘super-rotation’) is linearly stable for all Reynolds numbers. It is also known that a conducting fluid under the presence of a sufficiently strong axial electric current becomes unstable against nonaxisymmetric disturbances. It is thus suggestive that a super-rotation law may stabilize the rotating pinch. But for magnetic Prandtl number  $P_m \neq 1$  and for small magnetic Mach numbers of rotation also super-rotation *supports* the instability. For steeper and steeper rotation profiles the critical Hartmann numbers converge to a finite minimum value which for  $P_m \gg 1$  or  $P_m \ll 1$  loses its dependence on  $P_m$ . For super-rotation *and* for rigid rotation the sign of the azimuthal drift of the nonaxisymmetric hydromagnetic instability pattern strongly depends on the magnetic Prandtl number. The pattern corotates with the flow for  $P_m \geq 1$  and it counterrotates for  $P_m \ll 1$  so that a critical  $P_m$  exists (between 0.1 and 1) with solutions even resting in the laboratory system. On the other hand, for sub-rotation the instability pattern for all  $P_m$  migrates in the direction of the basic rotation. – An electric-current of (only) 3.6 kAmp suffices to realize the subcritical excitation for super-rotation in the laboratory using liquid sodium as the conducting fluid between the rotating cylinders.

PACS numbers: 47.65.Cb, 43.35.Fj, 62.60.+v

Keywords: Magnetic instability – differential rotation – Taylor-Couette flows

---

<sup>a)</sup>Electronic mail: gruediger@aip.de

## I. INTRODUCTION

A well-known instability of toroidal fields is the magnetohydrodynamical pinch-type current-driven instability which is basically nonaxisymmetric<sup>1</sup>. The toroidal field becomes unstable if a certain magnetic field amplitude is exceeded depending on the radial profile of the field which forms the electric current pattern. A global rotation of the system increases the critical field amplitude. It is strongly reduced, however, if the rotation decreases outwards (i.e.  $d\Omega/dR < 0$ , ‘sub-rotation’). The formal reason is that sub-rotation becomes (Rayleigh-) unstable even in the hydrodynamic regime if it is steep enough. More important is the existence of a nonaxisymmetric instability for such rotation laws even for current-free toroidal fields ( $B_\phi \propto 1/R$ ) which we have called azimuthal magnetorotational instability (AMRI<sup>2-4</sup>). It appears for rather low Hartmann numbers but for large magnetic Reynolds numbers of the basic sub-rotation. This phenomenon also explains the general destabilization of toroidal fields by rotation laws with  $\Omega$  *decreasing* outwards.

The question arises about the role of ‘super-rotation’ (i.e. rotation laws with  $d\Omega/dR > 0$ ) for which global AMRI solutions are not known so far. The super-rotation is also stable in the hydrodynamic regime<sup>5,6</sup>. The nonlinear behavior is less clear as some Taylor-Couette experiments have shown instability in this regime<sup>7,8</sup>. Superrotation cannot be destabilized by the standard magnetorotational instability. Inspired by the discovery of the axisymmetric helical MRI a WKB method for inviscid fluids in current-free helical background fields has been applied providing two limits of instability in terms of the shear in the rotation law<sup>9</sup>. An upper threshold suggests a magnetic destabilization of super-rotating flows but only for very strong positive shear. A similar phenomenon has been reported by Bonanno & Urpin (2008) resulting from a local analysis for a helical field under the influence of super-rotation<sup>10</sup>. Later it has been shown with a nonaxisymmetric dispersion relation for inductionless fluids that the stability curve does not cross the line representing the differentially rotating pinch formed by uniform electric-current which thus proves to be unstable for all signs of shear<sup>11</sup>. So far the upper limit of instability of MHD flows with positive shear is not yet confirmed as existing for real (i.e. diffusive) Taylor-Couette flows.

By means of a similar approximation Acheson showed that for fast-rotation the current-driven instability of toroidal fields may be stabilized by positive shear<sup>12</sup>. If this is true we expect in the solar low latitudes where in the bulk of the convection zone the equatorial  $\Omega$  increases outwards that the toroidal field is stabilized and can be amplified to much higher values than it would be true for

the opposite rotation law. Contrary to that a rotation law with negative shear – as it exists in higher latitudes – strongly destabilizes the fields so that they cannot reach high amplitudes. It is shown here by use of a simplifying cylinder geometry that indeed for not too small magnetic Prandtl numbers super-rotation stabilizes toroidal magnetic fields while sub-rotation strongly destabilizes toroidal magnetic fields. On the other hand, for small magnetic Prandtl number and for slow rotation both signs of  $d\Omega/dR$  lead to a subcritical excitation of the instability, so that for finite but small Reynolds number of the rotation the critical magnetic field strength becomes weaker than for the resting pinch.

A Taylor-Couette container is considered which confines a toroidal magnetic field with amplitudes fixed at the cylinders which rotate with different rotation rates. The gap between the cylinders is considered as variable. Normalized with the outer radius  $R_{\text{out}}$  the inner radius  $R_{\text{in}}$  is  $\geq 0.5$ . The cylinders are unbounded in axial direction.

The fluid between the cylinders is assumed to be incompressible and dissipative with the kinematic viscosity  $\nu$  and the magnetic diffusivity  $\eta$ . Derived from the conservation of angular momentum the rotation law  $\Omega(R)$  in the fluid is

$$\Omega(R) = a + \frac{b}{R^2} \quad (1)$$

with

$$a = \frac{\mu - r_{\text{in}}^2}{1 - r_{\text{in}}^2} \Omega_{\text{in}}, \quad b = \frac{1 - \mu}{1 - r_{\text{in}}^2} R_{\text{in}}^2 \Omega_{\text{in}}, \quad (2)$$

where

$$r_{\text{in}} = \frac{R_{\text{in}}}{R_{\text{out}}}, \quad \mu = \frac{\Omega_{\text{out}}}{\Omega_{\text{in}}}. \quad (3)$$

$\Omega_{\text{in}}$  and  $\Omega_{\text{out}}$  are the imposed rotation rates of the inner and outer cylinders. After the Rayleigh stability criterion the flow is hydrodynamically stable for  $\mu \geq r_{\text{in}}^2$ . We are only interested in hydrodynamically stable regimes so that  $\mu > r_{\text{in}}^2$  should be fulfilled. Rotation laws with  $d\Omega/dR > 0$  are described by  $\mu > 1$  while rotation laws with  $d\Omega/dR < 0$  are described by  $\mu < 1$ . Rigid rotation is described by  $\mu = 1$ . Hydrodynamical flows with rigid rotation or super-rotation are always linearly stable.

Also the possible magnetic profiles are restricted. The solution of the stationary induction equation without flows reads

$$B_\phi = AR \quad (4)$$

(in cylinder geometry, see Roberts 1956<sup>13</sup>, Tayler 1957<sup>14</sup>) where  $A$  corresponds to a uniform axial current everywhere within  $R < R_{\text{out}}$ . The quantity  $B_{\text{out}}/B_{\text{in}}$  measures the variation of  $B_\phi$  across the gap. For fields after (4) it is simply  $B_{\text{out}} = B_{\text{in}}/r_{\text{in}}$ .

The nonaxisymmetric AMRI is the result of the interplay of differential rotation (only for sub-rotation) and toroidal fields which are current-free in the conducting fluid. Here, the stability characteristics of the MHD system are only due to the pure Tayler instability (TI) for which we know that the magnetic threshold values for resting fluids do not depend the magnetic Prandtl number

$$\text{Pm} = \frac{\nu}{\eta}, \quad (5)$$

the value of which, however, has an essential influence on the excitation of the TI under the influence of rotation<sup>15,18</sup>. Both AMRI and (resting) TI have recently been realized in the MHD laboratory using the liquid eutectic alloy GaInSn with  $\text{Pm} = 1.4 \cdot 10^{-6}$  as the conducting fluid<sup>16,21</sup>. If the results shall be applied to turbulent media like the stellar convection zones then the magnetic Prandtl number must be replaced by its turbulence-induced values which are much larger<sup>19</sup>. In the upper part of the solar core the molecular value of the magnetic Prandtl number is about  $\text{Pm} \simeq 0.065$ <sup>20</sup>.

## II. EQUATIONS

The dimensionless incompressible MHD equations are

$$\begin{aligned} \text{Re} \frac{\partial \mathbf{u}}{\partial t} + \text{Re}(\mathbf{u} \cdot \nabla) \mathbf{u} &= -\nabla P + \Delta \mathbf{u} + \text{Ha}^2 \text{curl} \mathbf{B} \times \mathbf{B}, \\ \text{Rm} \frac{\partial \mathbf{B}}{\partial t} &= \text{Rm} \text{curl}(\mathbf{u} \times \mathbf{B}) + \Delta \mathbf{B}, \end{aligned} \quad (6)$$

with  $\text{div} \mathbf{u} = \text{div} \mathbf{B} = 0$  and with the Hartmann number

$$\text{Ha} = \frac{B_{\text{in}} D}{\sqrt{\mu_0 \rho \nu \eta}}. \quad (7)$$

$D = \sqrt{R_{\text{in}}(R_{\text{out}} - R_{\text{in}})}$  is used as the unit of length,  $\eta/D$  as the unit of velocity and  $B_{\text{in}}$  as the unit of magnetic fields. Frequencies including that of the global rotation  $\Omega$  are normalized with the inner rotation rate  $\Omega_{\text{in}}$ . The Reynolds number  $\text{Re}$  is defined as

$$\text{Re} = \frac{\Omega_{\text{in}} D^2}{\nu} \quad (8)$$

and the magnetic Reynolds number as  $R_m = P_m \text{Re}$ . It is also useful to work with the mixed Reynolds number  $\overline{R_m} = \sqrt{\text{Re}R_m}$  which is symmetric in  $\nu$  and  $\eta$  as it is the Hartmann number. Its ratio to (7) is called the magnetic Mach number  $M_m$  which measures the rotation rate in comparison with the Alfvén frequency  $\Omega_A = B_{\text{in}}/\sqrt{\mu_0\rho D^2}$ ,

$$M_m = \frac{\Omega_{\text{in}}}{\Omega_A}. \quad (9)$$

The boundaries are assumed as impenetrable and stress-free. The material of the cylinders is assumed as made from perfect conductors or in some other cases made from perfect insulators. The mathematical details about the boundary conditions and the used numerical codes can be found in previous publications<sup>17,18</sup>. Figures 1 summarize the influence of the differential rotation on the excitation of the current-driven instability against nonaxisymmetric modes with  $m = 1$ . The curves are for a gap with the inner cylinder at  $r_{\text{in}} = 0.8$  while the cylinders are isolating (blue lines) or perfect-conducting (red lines). The critical Hartmann numbers for resting cylinders are  $\text{Ha}_{\text{crit}} = 250$  for vacuum boundary conditions and  $\text{Ha}_{\text{crit}} = 290$  for perfect-conductor conditions. These values do not depend on the magnetic Prandtl number, as demonstrated here for the two examples with  $P_m = 1$  (left panel) and  $P_m = 10^{-5}$  (right panel). One finds that the Taylor instability with vacuum boundary conditions can be excited more easily than with perfect-conducting cylinders.

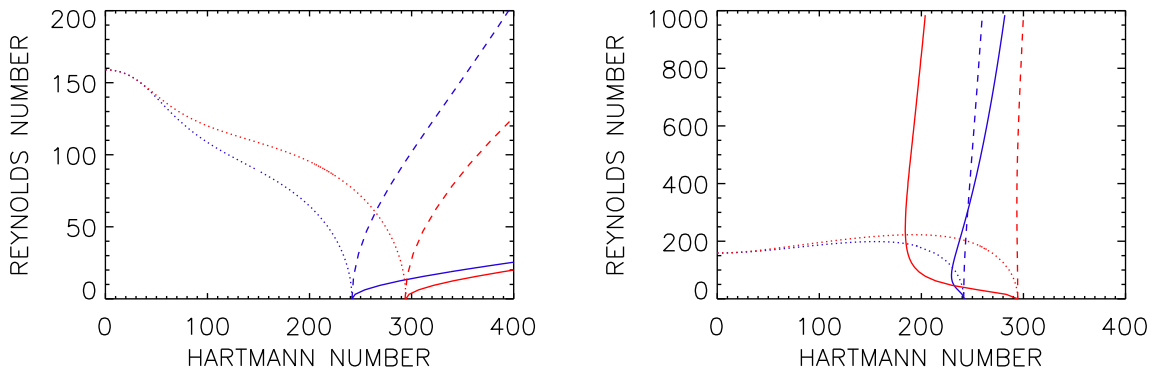


FIG. 1. Bifurcation map of the  $m = \pm 1$  mode for  $P_m = 1$  (left) and  $P_m = 10^{-5}$  (right) and for sub-rotation ( $\mu = 0.5$ , dotted lines), rigid rotation (dashed lines) and super-rotation ( $\mu = 4$ , solid lines). The colors represent the boundary conditions (vacuum: blue; perfect conductor: red).  $r_{\text{in}} = 0.8$ .

The dashed lines describe the influence of rigid rotation which always acts stabilizing, i.e.  $d\text{Re}/d\text{Ha} > 0$ . This effect, however, is much weaker for small  $P_m$  than for  $P_m = 1$ . In the latter

case the instability is suppressed already for very slow rotation. In both cases the rigid rotation *stabilizes* the Tayler instability. The stabilization depends on the value of the magnetic Prandtl number. It is strongest for  $P_m = 1$ . For  $P_m < 1$  or  $P_m > 1$  (not shown) the rotational influence on the onset of the instability becomes weaker and weaker.

The solid lines represent rotation laws with positive radial shear. Their behavior strongly depends on the value of the magnetic Prandtl number. For  $P_m = 1$  (left panel) super-rotation ( $\mu = 4$ ) acts stabilizing ( $dRe/dHa > 0$  everywhere) while for small magnetic Prandtl number ( $P_m = 10^{-5}$ , right panel) it acts destabilizing ( $dRe/dHa < 0$  in the lower part of the diagram). The dotted lines in Fig. 1 are for the rotation law with  $\mu = 0.5$ . In the narrow gap and for fast enough rotation such a rotation law is linearly unstable without magnetic field. The magnetic field even destabilizes such a steep rotation law so that for finite Hartmann number the critical Reynolds number is always lower than 160 which is the critical value for  $Ha = 0$ . The influences of the boundary conditions and the magnetic Prandtl number on the stability of sub-rotation laws is only small.

The subcritical excitation of the TI by super-rotation is insofar interesting as TC-flows with positive shear are prominent examples of stable flows<sup>6</sup>. Such a very stable configuration can obviously be destabilized by a weak axial current which is weaker than the critical electric-current for the TI with resting cylinders. This phenomenon only exists for slow rotation as for fast rotation all nonaxisymmetric magnetic instabilities are suppressed by any sort of differential rotation. The magnetic Mach number  $M_m$  for the subcritical excitation by super-rotation in the right panel of Fig. 1 is (only) of order  $10^{-3}$ . Note that a rotation profile with  $\mu > 1$  needs much higher magnetic fields to be destabilized than a rotation law with  $\mu < 1$ . With other words, the toroidal field which is induced by a super-rotation can become much stronger than the toroidal field which is induced by a sub-rotating  $\Omega$ -profile. This basic finding should have implications for the electrodynamics of rotating stars.

The latter finding is indeed repeated by our numerical solutions for  $P_m \neq 1$ . In the following we shall consider in more detail the TC-flows with a very narrow gap ( $r_{in} = 0.95$ ) and the standard gap with  $r_{in} = 0.5$ .

### III. NARROW GAP

For a narrow gap the influence of the magnetic Prandtl number on the Tayler instability in a container with various rotation profiles shall be studied. All the considered rotation laws are hydrodynamically stable. For a gap with  $r_{\text{in}} = 0.95$  Fig. 2 gives the results for  $P_m = 0.1$ ,  $P_m = 1$  and  $P_m = 10$ . The critical Hartmann number for TI is  $Ha_{\text{crit}} = 3060$ . For  $P_m = 1$  rigid-body rotation and super-rotation of any Reynolds number are always supercritical, i.e.  $Ha > 3060$ . As known, only sub-rotation leads to subcritical excitations. However, the differences for both sub-rotation and for super-rotation here only appear for rather high Reynolds numbers. For the outer part of the solar convection zone the magnetic Reynolds number does not exceed (say) 300. For younger solar-type stars it can easily reach the high value of 2000.

We find super-rotation as always stabilizing but as we shall demonstrate this is only true for  $P_m = 1$ .

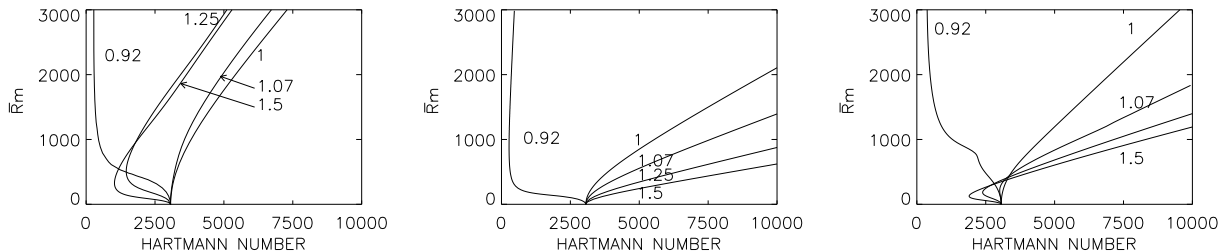


FIG. 2. Stabilization and destabilization by super-rotation in a narrow gap for  $P_m = 10$  (left),  $P_m = 1$  (middle) and  $P_m = 0.1$  (right). The curves are marked with their value of  $\mu$ .  $r_{\text{in}} = 0.95$ , conducting boundaries.

#### A. Subcritical excitations

These findings are not confirmed if  $P_m \neq 1$ . It makes sense for better comparison to use the modified Reynolds number  $\overline{Rm}$  for the characterization of the basic rotation. For both  $P_m > 1$  (Fig. 2, left panel) and  $P_m < 1$  (Fig. 2, right panel) also the rotation laws with positive shear lead to subcritical excitations if the rotation is slow enough. The magnetic Mach number which measures the rotation of the (inner) cylinder to the Alfvén frequency for the subcritical excitation and for both magnetic Prandtl numbers is  $Mm \simeq 0.05$ . For sufficiently fast rotation also the super-

rotation laws are stabilizing. The super-rotation for small magnetic Prandtl numbers is much more stabilizing than that for high magnetic Prandtl numbers. For  $P_m = 10$  the stabilization by super-rotation is even weaker than that of rigid rotation. It is often the rule in the theory of magnetic instabilities that large  $P_m$  destabilize nonuniform rotation while small  $P_m$  stabilize the flows. The formal reason for this phenomenon can be realized in Fig. 1 where the bifurcation curve for super-rotation for small  $P_m$  moves to the left of the line for rigid rotation rather than to the right as for  $P_m = 1$ .

It is known that rotation laws with negative shear (here  $\mu = 0.92$ ) behave strongly destabilizing the flow. The domain of stability in Fig. 2 is again larger for small  $P_m$ . For sufficiently fast rotation also the lines of marginal instability for sub-rotation turn to the right stabilizing the system as rotation laws of any shear do always erode nonaxisymmetric magnetic patterns.

The question arises about the possible existence of a minimum Hartmann number for steeper and steeper super-rotation laws. The existence of such a limit is suggested by the suppression of a nonaxisymmetric magnetic field by differential rotation which should grow with growing values of shear. The line of marginal instability can never touch the vertical axis as in the hydrodynamic regime super-rotation always behaves stable. Figure 3 indeed shows very close lines for  $\mu = 4$  and  $\mu = 8$  so that one can estimate that the minimum Hartmann number  $Ha_{\text{Min}}$  which can be reached with super-rotation is smaller by a factor of three compared with the Taylor instability value  $Ha_{\text{crit}} = 3060$ . For the very small magnetic Prandtl number used for Fig. 3 the numerical value of  $Ha_{\text{Min}}/Ha_{\text{crit}}$  is astonishing small. Below we shall discuss the dependencies of the magnetic-field reduction by super-rotation on the gap-width and on the  $P_m$  value in more detail.

## B. Pattern migration

Figure 4 shows the behavior of the azimuthal migration of the nonaxisymmetric vortices as much more complicated. The drift rate  $\omega_{\text{dr}}$  is the real part of the frequency of the Fourier mode  $\exp(i(\omega t + m\phi))$  of the instability, now normalized with the rotation rate of the *outer* cylinder. They can be positive or negative, it is also striking that for large  $P_m$  or for sub-rotation often  $|\omega_{\text{dr}}| \simeq \Omega_{\text{out}}$ . Because of the definition

$$\dot{\phi} = -\frac{\omega_{\text{dr}}\Omega_{\text{out}}}{m} \quad (10)$$

( $\omega_{\text{dr}}$  the real part of the azimuthal Fourier frequency of the mode) the azimuthal migration has the opposite sign of  $\omega_{\text{dr}}$ . It is also important to know that the solutions for the modes with  $m = 1$



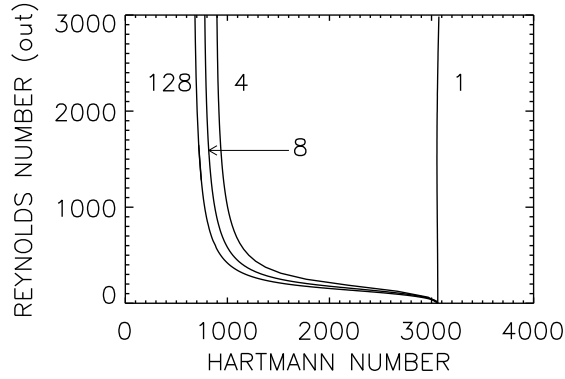


FIG. 3. Bifurcation map for super-rotation, the lines are marked with their value of  $\mu$ .  $r_{\text{in}} = 0.95$ ,  $\text{Pm} = 10^{-5}$ . The Reynolds number is calculated with the *outer* rotation rate. Conducting boundaries.

and  $m = -1$  have the same eigenvalues  $\text{Re}$  and  $\text{Ha}$  but the opposite signs of  $\omega_{\text{dr}}$ . After (10) they have thus the same frequency of migration in  $\phi$ -direction. Generally, both modes with  $m = \pm 1$  are simultaneously excited. If the pinch rotates rigidly,  $\mu = 1$ , then both modes have exactly the same amplitudes and form a standing wave. The instability pattern looks kidney-shaped with the drift direction depending on the magnetic Prandtl number. Note also the nearly circular geometry of the resulting cells in the  $R$ - $z$ -plane (Fig. 5). For a certain  $\text{Pm}$  between 0.1 and 1 the azimuthal migration disappears and the entire pattern will rest in the laboratory.

For nonuniform rotation laws with finite shear one of the modes  $m = 1$  or  $m = -1$  is preferred and the kidney-structure becomes a spiral. From Fig. 4 we also find that the nonaxisymmetric instability pattern for sub-rotation nearly corotates with the outer cylinder (as it is observed for AMRI, see<sup>4,16</sup>) for all magnetic Prandtl numbers. For  $\text{Pm} \gtrsim 1$  the drift frequencies for super-rotation are negative, too, so that also their magnetic pattern azimuthally migrates in the direction of the rotation. This is in particular true for the case of uniform rotation.

For smaller magnetic Prandtl numbers, however, for rigid rotation and for super-rotation the pattern counter-rotates. The azimuthal migration of the linear solutions directly reflects the actual value of the magnetic Prandtl number. Simulation solutions with magnetic Prandtl numbers of order unity for flows with vanishing or positive shear may easily lead to results which are not representative for smaller  $\text{Pm}$ . On the other hand, rotation laws with negative shear do not show that sensitivity to the  $\text{Pm}$ -value (see also Fig. 7, below).

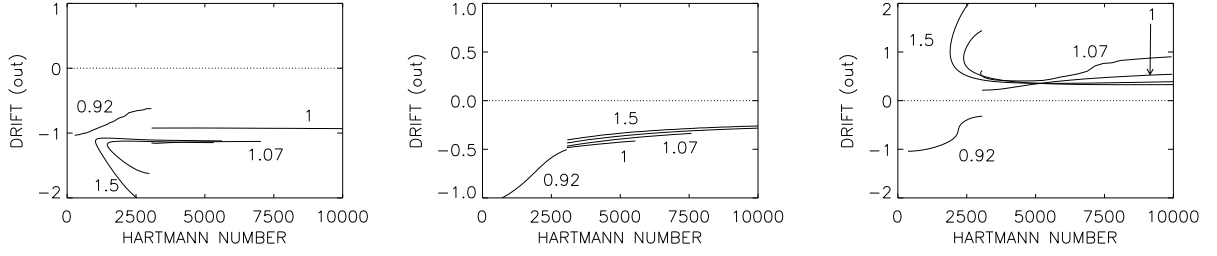


FIG. 4. The same as in Fig. 2 but for the normalized drift frequency in a narrow gap ( $r_{in} = 0.95$ ) for  $P_m = 10$  (left),  $P_m = 1$  (middle) and  $P_m = 0.1$  (right). The values are normalized with  $\Omega_{out}$  (see Eq. (10)). Conducting boundaries.

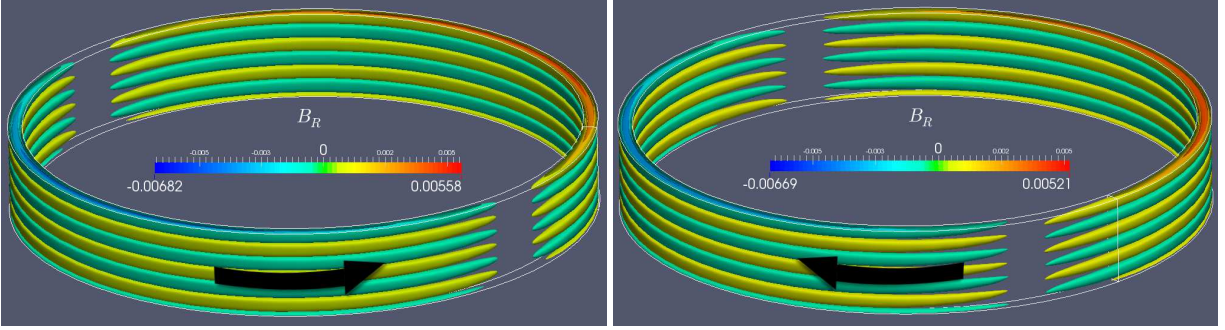


FIG. 5. Rigid rotation: the isolines of the  $b_R$  in a narrow gap for  $P_m = 1$  (left) and  $P_m = 0.1$  (right). Both modes with  $m = \pm 1$  are excited with the same amplitude forming a standing wave. The pattern with  $P_m = 1$  migrates in the same direction as the rotational motion while for  $P_m = 0.1$  it migrates opposite.  $r_{in} = 0.95$ ,  $\mu = 1$ ,  $Re = 111$ ,  $Ha = 3440$ , conducting boundaries.

#### IV. WIDE GAP

For a wide gap with  $r_{in} = 0.5$  Fig. 6 gives the Reynolds numbers and drift rates for *uniform* rotation in their dependence on the magnetic Prandtl number. Again the dashed line in the left panel shows a very strong stabilization effect by the rotation for  $P_m = 1$  and a very weak instability suppression for much smaller  $P_m$ . The drift curves are similar for all gap widths. It is a basic result that the instability pattern for uniform rotation corotates with the cylinders for  $P_m \geq 1$  and it counterrotates for  $P_m \leq 0.1$ . For a certain value of  $P_m$  between 0.1 and 1 the drift vanishes and the pattern rests in the laboratory system. The observation of the rotating magnetic pattern will thus only lead to conclusions about the rotation of the plasma if the magnetic Prandtl number is known.

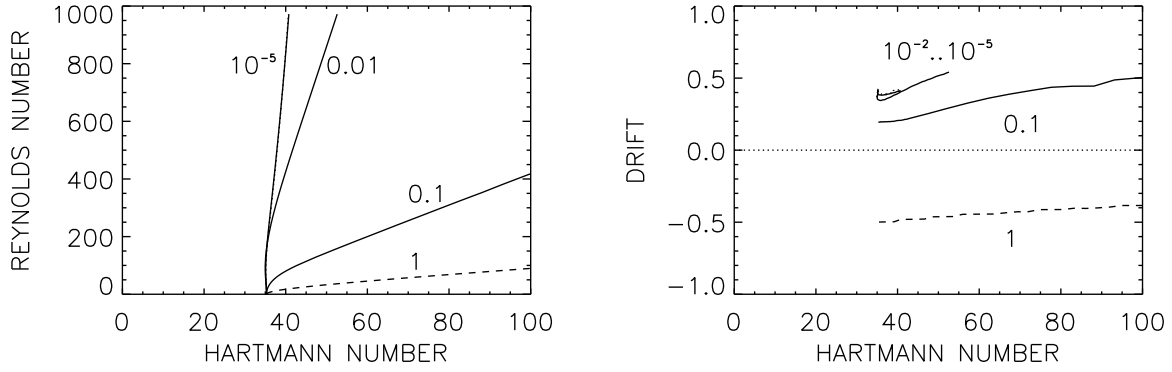


FIG. 6. Rigid rotation: the Reynolds numbers (left panel) and the normalized drift frequency (right panel) in a gap with  $r_{\text{in}} = 0.5$  for various  $\text{Pm}$ :  $\text{Pm} = 1$  (dashed),  $\text{Pm} = 10^{-1}$ ,  $\text{Pm} = 10^{-2}$ ,  $\text{Pm} = 10^{-3}$ ,  $\text{Pm} = 10^{-5}$  (all solid). Conducting boundaries.

### A. Instability map

In advance to a possible laboratory experiment the Figs. 7 give the eigenvalues for marginal instability for a container with  $r_{\text{in}} = 0.5$  and for the magnetic Prandtl number of  $\text{Pm} = 10^{-5}$  for liquid sodium. The characteristic Hartmann number for conducting boundaries and for resting cylinders is  $\text{Ha}_{\text{crit}} = 35.3$  independent of the value of the magnetic Prandtl number<sup>15</sup>. Reynolds number and drift rate are related from now on to the rotation rate of the *outer* cylinder.

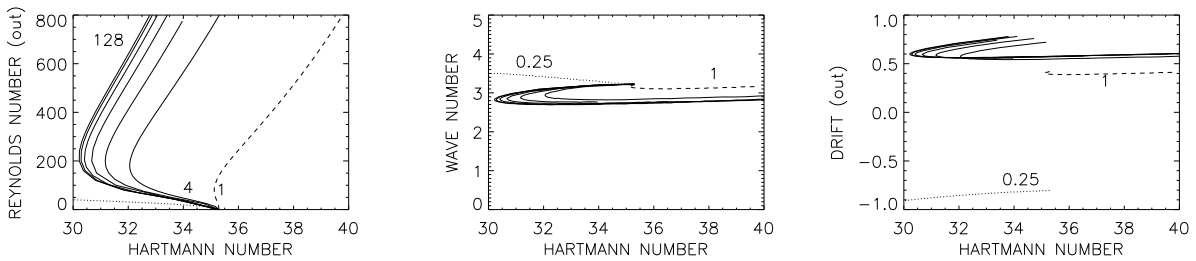


FIG. 7. Left: Instability map for super-rotation in a wide gap, the lines are marked with  $\mu$ . The dashed curve represents the stabilization effect of rigid rotation while the dotted curve shows for comparison the result for  $\mu = 0.25$ , i.e. the Rayleigh limit. Middle: Wave numbers. Right: Drift rates.  $r_{\text{in}} = 0.5$ ,  $\text{Pm} = 10^{-5}$ , conducting cylinders.

Figure 7 (left) shows the curves of marginal instability for many rotational laws with  $\mu$  between 1 and 128. The subcritical excitation of the current-driven instability by super-rotation can clearly

be realized, the curves are converging if the Reynolds number is formed with the outer rotation rate,  $\text{Re}_{\text{out}} = \mu \text{Re}$ . However, a minimum Hartmann number of order 30 exists which cannot further be reduced by steeper rotation laws. It is also clear that for  $\text{Re}_{\text{out}} > 200$  the differential rotation starts to suppress the nonaxisymmetric instability.

It is not complicated to realize a Hartmann number of order 30 for a container with  $r_{\text{in}} = 0.5$  in a laboratory. The necessary current in the gap to produce a certain Hartmann number  $\text{Ha}$  is

$$I_{\text{fluid}} = 5 \sqrt{\frac{(1 - r_{\text{in}})(1 + r_{\text{in}}^2)}{r_{\text{in}}^3}} \sqrt{\mu_0 \rho \nu \eta} \text{Ha}, \quad (11)$$

(Rüdiger et al. 2013<sup>18</sup>). It is  $\sqrt{\mu_0 \rho \nu \eta} \simeq 8.2 \text{ G}\cdot\text{cm}$  for liquid sodium. To reach  $\text{Ha} = 30$  one needs thus an electric-current of 3.6 kAmp flowing through the sodium. For the narrow gaps with  $r_{\text{in}} = 0.95$  considered below this minimum value grows to about 15 kAmp.

The axial wave numbers are plotted in the middle panel of Fig. 7. From the definitions follows

$$\frac{\delta z}{D} \simeq \frac{\pi}{k} \sqrt{\frac{R_{\text{in}}}{D}} \quad (12)$$

so that  $\delta z/D \simeq \pi/k$  for the considered container. The data lead to  $\delta z \simeq D$  what means that the Taylor cells approximately form a circle in the  $R$ - $z$  plane. This result does also not depend on the gap width.

In Fig. 7 (right) the drift rates of the induced instability pattern are given. We again find all drift rates for rigid rotation and super-rotation are positive as they are for rigid rotation and small magnetic Prandtl number. For steep sub-rotation laws (here  $\mu = 0.25$ , the Rayleigh limit) the drift rates are negative. Note that for  $\omega_{\text{dr}}/\Omega_{\text{out}} = -1$  the magnetic pattern strictly corotates-rotates with the outer cylinder. In contrast, the magnetic pattern for *all* super-rotation laws including uniform rotation migrates opposite to the sense of rotation corresponding to the behavior of the drift rates in the narrow gap (Fig. 4, right). For rotation laws with non-negative shear the sign of the azimuthal migration reflects the value of the magnetic Prandtl number. For small  $\text{Pm}$  by choice of the rotation rate of the outer cylinder one can obtain all sorts of migration of the magnetic pattern between corotation and counterrotation.

## B. Growth rates

The subcritical excitation of the TI for rotation laws with positive shear only exists for sufficiently slow rotation ( $\text{Mm} \simeq 0.02$ ) so that the instability only grows very slowly as Fig. 8

demonstrates for super-rotation. The growth rates are normalized with the outer rotation rate. Doing so the maximum growth rates always occur at the same Reynolds number. For the upper curve of the plot one finds that  $\omega_{\text{gr}} \simeq 0.03\Omega_{\text{out}}$  for  $\text{Re} \simeq 130$  so that the exponential growth time is  $\tau_{\text{gr}} \simeq 10R_{\text{out}}^2$  in seconds when  $R_{\text{out}}$  is measured in cm ( $\nu = 7 \cdot 10^{-3} \text{ cm}^2/\text{s}$  for liquid sodium). If the expression

$$\omega_{\text{gr}} = \Gamma \frac{B_{\text{out}}^2}{\mu_0 \rho \eta} \quad (13)$$

for the growth rate is adopted, which has been derived for the nonrotating pinch and which has been experimentally realized<sup>15,21</sup>, then for the strongest super-rotation the Fig. 8 gives  $\Gamma \simeq 10^{-3}$  which well fits the theoretical results for resting container. It certainly can be increased for wider gaps but the exponential growth time of the instability for slow super-rotation will hardly be shorter than that for the resting pinch.

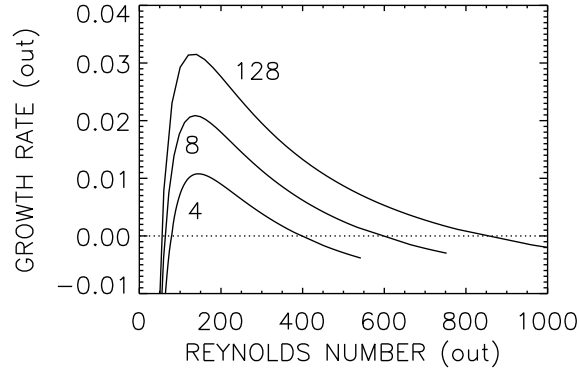


FIG. 8. Growth rates for  $\text{Ha} = 33$  with  $\mu = 4, 8,$  and  $128$ .  $r_{\text{in}} = 0.5$ ,  $\text{Pm} = 10^{-5}$ , conducting cylinders.

## V. A LOCAL APPROXIMATION

The described effects have mainly been demonstrated by means of the boundary conditions which are valid for perfect-conducting cylinders. After Fig. 1 the negative slope  $d\text{Re}/d\text{Ha} < 0$  of the lines of marginal instability for *slow* rotation also exists for models with vacuum conditions but with reduced efficiency. It is thus worthwhile to discuss the result

$$\text{Re}^{*2} = \frac{1}{4} \frac{((1 + \text{Ha}^{*2} m^{*2})^2 - 4\text{Ha}^{*4} m^{*2})(1 + \text{Ha}^{*2} m^{*2})^2}{\text{Ha}^{*4} \text{Ro}^2 m^{*2} - (\text{Ro} + 1)((1 + \text{Ha}^{*2} m^{*2})^2 - 4\text{Ha}^{*4} m^{*2})}, \quad (14)$$

of a local approximation for  $Pm \rightarrow 0$  where  $Re^*$ ,  $Ha^*$  and  $m^*$  represent the slightly modified Reynolds number, Hartmann number and azimuthal wave number<sup>22</sup>. The Rossby number  $Ro = (1/2)d\log\Omega/d\log R$  represents the differential rotation, it is positive for super-rotation and negative for sub-rotation. In contrast to all other quantities the Rossby number enters the Eq. (14) with odd and even powers. In (14) the  $Ro$  must be independent of the radius  $R$  which approximately complies with Taylor-Couette flows of weak sub-rotation and of weak super-rotation, i.e.  $0.2 < \mu < 2$ . The latter super-rotation law corresponds with  $Ro \simeq 1$  in a good approximation.

We shall show that all curves with  $m^* > 1$  in a  $Ha^*$ - $Re^*$  plane for slow rotation show a subcritical behaviour compared with the critical eigenvalue  $Ha_{crit}^* = 1/\sqrt{m^*(2-m^*)}$  for  $Re^* = 0$ , i.e.  $Ha^*(Re^*) < Ha_{crit}^*$ . To this end the function  $Z = (1 + Ha^{*2}m^{*2})^2 - 4Ha^{*4}m^{*2}$  is defined so that (14) yields

$$Z = \frac{4Re^{*2}Ha^{*4}Ro^2m^{*2}}{(1 + Ha^{*2}m^{*2})^2 + 4(Ro + 1)Re^{*2}}. \quad (15)$$

Obviously, the function  $Z(Re^*)$  only vanishes for  $Re^* = 0$  and it is positive-definite for finite  $Re^*$  if – as we shall assume –  $Ro > -1$ . The above mentioned eigenvalue  $Ha_{crit}^*$  forms the solution of  $Z = 0$ . It only exists for  $m^* < 2$ . The solution of  $Z = \delta$  with  $\delta > 0$  can thus be written as  $Ha^{*2} = Ha_{crit}^{*2} + \varepsilon$  with unknown sign of  $\varepsilon$  which, without loss of generality, can be assumed as small against  $Ha_{crit}^*$ . Hence, from the definition of the function  $Z$  follows

$$\varepsilon = -\frac{\delta}{4m^*}, \quad (16)$$

so that always  $\varepsilon < 0$ . For  $Ro > -1$  it is thus  $Ha^*(Re) < Ha_{crit}^*$  for negative and positive shear, i.e. the excitation of the Tayler instability becomes always subcritical by the action of any differential rotation. It is possible to demonstrate that this result does not change without the restriction to small  $\varepsilon$ .

The fact that  $Z = 0$  requires  $Re^* = 0$  has the consequence that  $Ha^* = Ha_{crit}^*$  does not appear as a solution of (14) for finite Reynolds numbers. Hence, the curves of marginal instability always remain in the subcritical domain with  $Ha^*(Re^*) < Ha_{crit}^*$  and never reach Hartmann numbers larger than  $Ha_{crit}^*$ . The suppression of the Tayler instability by fast rotation (see Fig. 7) is thus not reflected by the local relation (14) for inductionless fluids.

## VI. SUMMARY

A rotating pinch with a homogeneous axial electric current has been considered where the cylindrical bounding walls rotate with  $\mu \geq 1$ , i.e. the outer cylinder rotates with the same rotation rate or rotates faster than the inner cylinder. A linear perturbation theory fixes the critical Hartmann numbers for which the system becomes marginally unstable. The surprising result is that for slow rotation with  $\Omega_{\text{out}} \ll \Omega_A$  the excitation of the nonaxisymmetric perturbations becomes subcritical so that the critical Hartmann number for rotation is smaller than without rotation. It is numerically shown that for steeper rotation laws the series of minimum Hartmann numbers converge to a total minimum  $\text{Ha}_{\text{Min}}$  for  $\mu \rightarrow \infty$  (approaching resting inner cylinders). The resulting excitation relief

$$\chi = \frac{\text{Ha}_{\text{crit}} - \text{Ha}_{\text{Min}}}{\text{Ha}_{\text{crit}}} \quad (17)$$

depends on the magnetic Prandtl number  $\text{Pm}$ . It vanishes for  $\text{Pm} = 1$  and takes similar values for very large and for very small  $\text{Pm}$ . Subcritical easings of order 20% ( $r_{\text{in}} = 0.5$ ) and 80% ( $r_{\text{in}} = 0.95$ ) exist for  $\text{Pm} \neq 1$  (Fig. 9, left).

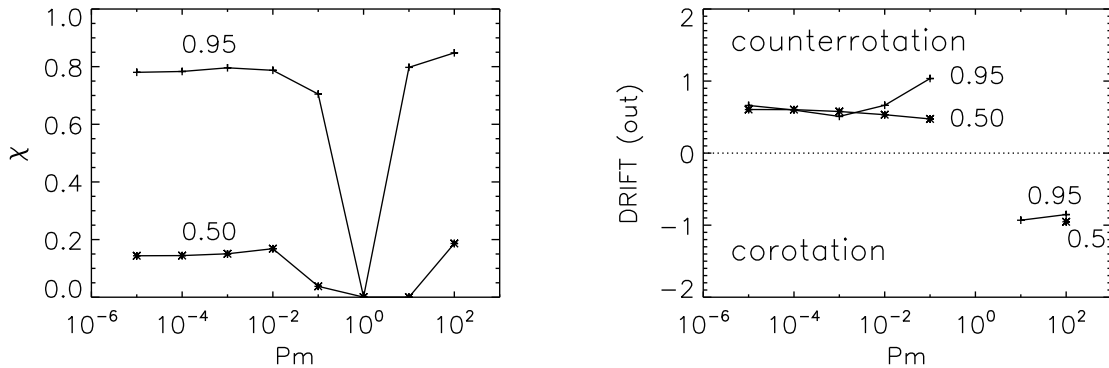


FIG. 9. The influence of the magnetic Prandtl number on the maximal reduction of the Hartmann number (left) and the related drift frequencies  $\omega_{\text{dr}}$  (right). For  $\text{Pm} \gg 1$  and for  $\text{Pm} \ll 1$  the subcritical excitation measured by (17) is similar but the signs of the azimuthal migration of the instability pattern differ. The curves are marked with  $r_{\text{in}}$ ,  $\mu \rightarrow \infty$ , conducting boundaries.

The instability for  $\text{Pm} \gg 1$  and for  $\text{Pm} \ll 1$  differs in another respect. For sub-rotation we always find that the pattern migrates for all  $\text{Pm}$  in positive direction of the azimuthal coordinate  $\phi$ . For solid-body rotation and for super-rotation there is, however, a strong influence of the magnetic Prandtl number on the azimuthal migration of the perturbation patterns. For  $\mu \geq 1$

the pattern counterrotates for small  $P_m$  while it corotates for  $P_m \gtrsim 1$ . Hence, a critical  $P_m$  exists for which the pattern rests in the laboratory system. The  $P_m$ -dependence of the drift frequency  $\omega_{dr}$  disappears for small and for large magnetic Prandtl numbers (Fig. 9, right panel). The latter finding is also true for a pinch with solid-body rotation.

## ACKNOWLEDGMENTS

This work was supported in frame of the Helmholtz Alliance LIMTECH, as well as by Deutsche Forschungsgemeinschaft under SPP 1488 (PlanetMag).

## REFERENCES

- <sup>1</sup>R. J. Tayler, Mon. Not. R. Astron. Soc. **161**, 365 (1973).
- <sup>2</sup>G. Rüdiger, R. Hollerbach, M. Schultz, et al. , Mon. Not. R. Astron. Soc. **377**, 1481 (2007).
- <sup>3</sup>R. Hollerbach, V. Teeluck, and G. Rüdiger, Phys. Rev. Lett. **104**, 44502 (2010).
- <sup>4</sup>G. Rüdiger, M. Gellert, M. Schultz M., R. Hollerbach, and F. Stefani, Mon. Not. R. Astron. Soc. **438**, 271 (2014).
- <sup>5</sup>G.I. Taylor, Proc. Roy. Soc. London **157**, 546 (1936).
- <sup>6</sup>F. Schultz-Grunow, Z. Angewandte Mech. **39**, 101 (1959).
- <sup>7</sup>D. Borrero-Echeverry, M.F. Schatz and R. Tagg, Phys. Rev. E **81**, 25301 (2010).
- <sup>8</sup>M.J. Burin and C.J. Czarnocki, J. Fluid Mech. **79**, 106 (2012).
- <sup>9</sup>W. Liu, J. Goodman, I. Herron et al., Phys. Rev. E, **74**, 056302 (2006).
- <sup>10</sup>A. Bonanno and U. Urpin, Astron. Astrophys. **488**, 1 (2008).
- <sup>11</sup>O. Kirillov and F. Stefani, Phys. Rev. Lett. **111**, 062203 (2013).
- <sup>12</sup>D.J. Acheson, Philos. Trans. Roy. Soc. A **289**, 459 (1978).
- <sup>13</sup>P.H. Roberts, Astrophys. J. **124**, 430 (1956).
- <sup>14</sup>R.J. Tayler, Proc. Phys. Soc. B **70**, 31 (1957).
- <sup>15</sup>G. Rüdiger and M. Schultz, Astron. Nachr. **331**, 121 (2010).
- <sup>16</sup>M. Seilmayer, V. Galindo, G. Gerbeth, et al., Phys. Rev. Lett. **113**, 024505 (2014).
- <sup>17</sup>M. Gellert, G. Rüdiger, and A. Fournier, Astron. Nachr. **328**, 1162 (2007).
- <sup>18</sup>G. Rüdiger, L.L. Kitchatinov and R. Hollerbach, *Magnetic Processes in Astrophysics: Theory, Simulations, Experiments*, Wiley-VCH, Berlin (2013).



- <sup>19</sup>T.A. Yousef, A. Brandenburg, and G. Rüdiger, *Astron. Astrophys.* **411**, 321 (2003).
- <sup>20</sup>D.O. Gough, in *The Solar Tachocline*, (eds. D. Hughes, R. Rosner and N. Weiss), Cambridge University Press (2003).
- <sup>21</sup>M. Seilmayer, F. Stefani, T. Gundrum, et al., *Phys. Rev. Lett.* **108**, 244501 (2012).
- <sup>22</sup>O. Kirillov, F. Stefani, and Y. Fukumoto, *J. Fluid Mech.* **760**, 591 (2014).